Simplified Field-Oriented Control Algorithm Implementation on 1.15 MW Traction System

Constantin Vlad Suru[*], Tudor Mătușa[†], Mihaela Popescu[*] and Alexandru Bitoleanu[*]
[*] University of Craiova/Department of Electromechanics, Environment and Applied Informatics, Craiova, Romania, vsuru@em.ucv.ro, mpopescu@em.ucv.ro, a_bitoleanu@yahoo.com,
ORCID: 0000-0002-2839-1686, 0000-0002-5292-5529, 0000-0001-9621-5011
[†] Promat SA, Craiova, Romania, matusa.tudor.e8y@student.ucv.ro, ORCID: 0009-0006-7263-547X

Abstract **- The purpose of this work is the implementation and experimental validation of a quasi-oriented rotor flux control algorithm on a full scale, railway locomotive traction system. This control method can be useful for industrial applications based on DSPs which have limited computation power, given the fact that the real time flux-oriented control needs relatively high computation power, especially for the flux estimator. The advantage of this method is given by the elimination of flux estimation as it assumes the control system is oriented. This way, a processor hungry control section is avoided, the flux control loop being also avoided. The control algorithm had been implemented in the Matlab Simulink environment, using the dSPACE RTI toolbox, for the DS1103 prototyping board. The dSPACE board had been used for the control of the full-scale traction system experimental stand.**

Cuvinte cheie: *control cu orientare după câmp, sistem de tracțiune, control cu DSP.*

Keywords: *field-oriented control, traction system, DSP control.*

I. Introduction

For its known advantages, the induction motor is widely used for the traction system of modern rail vehicles [1][2][3][4]. Irrespective to the vehicle traction power, the traction system is equipped with multiple relatively large power induction motors. The control of the traction system is assured by a DSP [5]. For the most railway vehicles, the power inverter is fed from the overhead catenary by means of a power transformer and bidirectional rectifier (necessary to recover the braking energy to the power grid. A new type of railway vehicles is the battery fed locomotives which can recover the braking energy by charging the battery [6]. The disadvantage of induction motor traction systems is given by the relatively complex and computing hungry closed loop control system. An example of such a control system is the rotor field-oriented control algorithm which can give good results, but which needs the estimation of the motor flux [4][5]. The flux estimator is sensitive to computing error; therefore, it needs a high-performance DSP which can give a sufficiently small sample time [7][8].

Another limitation of such systems is the relatively low switching frequency of the power inverter transistors which leads to high current ripple.

The prototyping systems are characterized by high computing power (as dSPACE DS1103, for example [9]), but industrial DSPs have limited computing power, which means that the sample time is inevitably higher for the latter. High sample time values lead to cumulative computing errors which can further lead to instable and peculiar system response, different than the response defined by the equations [7].

An alternative to a small sample time is a simpler control algorithm, obtained by eliminating the flux estimator and assuming that the control system is oriented. The control algorithm becomes quasi-oriented, which had been validated on a small-scale experimental system [10].

After the introduction, the simplified, quasi-oriented control algorithm is briefly described in the second section, and its implementation is presented in the third section. The experimental setup is described in the fourth section and the experimental results are discussed in the sixth section. Finally, the conclusions are drawn.

II. Simplified Rotor Field Oriented Control Algorithm

For the rotor field-oriented control, the motor currents are computed in a rotating referential (d-q) which is synchronized with the rotor flux. Because the flux estimator is no longer used, the rotor flux is now unknown, so the algorithm uses the assumption that the system is oriented. The advantage is given by the fact that the flux estimator is not used. This implies that the flux controller can be eliminated also. The disadvantage is given by the fact that the active and magnetizing motor current components cannot be regulated separately (on the d and q axes) but commonly, by regulating the motor current magnitude [10].

The simplified control is illustrated in Fig. 1 [10], where:

- $|I_m|$ - motor current magnitude computation block;
- R_i - motor current magnitude controller;
- VSI - voltage source inverter;
- $\approx$ - Sinusoidal control signals generator;
- f_2^* - slip frequency computation block.

The algorithm inputs are the imposed rotor flux and the imposed motor speed. For a given flux value, assuming that the control system is oriented, the imposed magnetizing current is [12][10]:

$$i_{sd} = \frac{1}{L_m} \cdot \left(\Psi_{rd} + T_r \cdot \frac{d\Psi_{rd}}{dt} \right) \qquad (1)$$

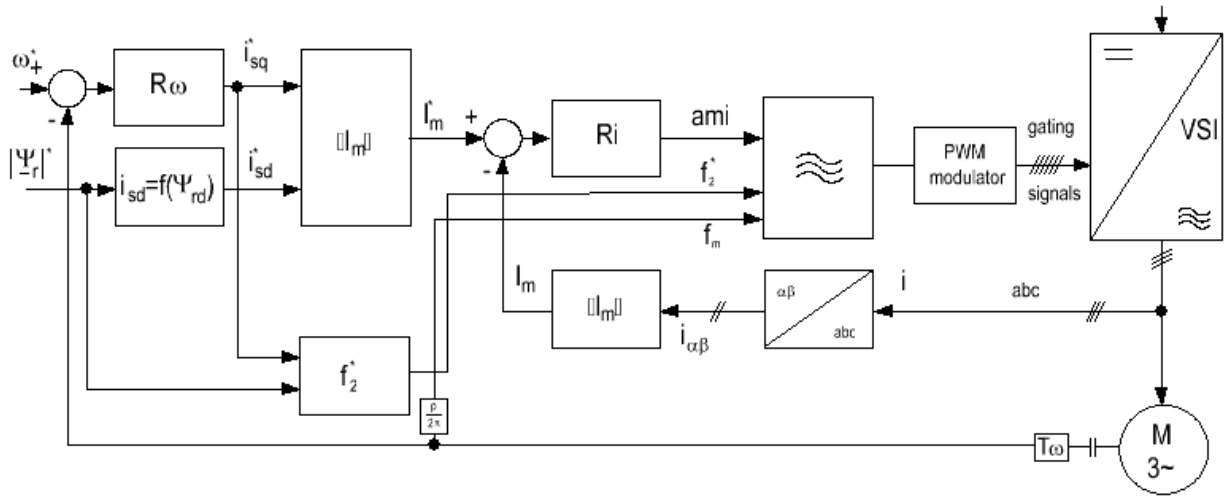

Fig. 1. Block diagram of the simplified field-oriented control algorithm

where:

- L_m - magnetizing inductance;
- Ψ_{rd} - rotor flux on d axis or the referential;
- T_r - rotor circuit time constant:

$$T_r = \frac{L_r}{R_r} = \frac{L_m + L_{\sigma r}}{R_r} \tag{2}$$

- $L_{\sigma r}$ - rotor leakage inductance;
- R_r - rotor resistance.

The active current (q axis) is obtained at the output of the speed controller.

The imposed active and magnetizing currents are used for the magnitude of the imposed motor current phasor, which is regulated by a proportional-integrative regulator (Fig. 1):

The feedback quantity of the current magnitude controller is the real motor current phasor magnitude (computed from the sampled stator currents in the stationary reference frame [1][7], using the Clarke transform.

The current magnitude controller gives the amplitude modulation index ("ami" in Fig. 1) for the three-phase sinusoidal control voltages, software generated based on the motor frequency and slip frequency. The slip frequency is computed considering the imposed active current, and flux [12]:

$$f_2^* = i_{sq} \cdot \frac{L_m}{2 \cdot \pi \cdot \Psi_{rd} \cdot T_r} \tag{3}$$

The software generated control voltages are applied to the sinusoidal PWM modulator.

III. Simplified Rotor Field Control Algorithm Implementation

The control algorithm has been experimentally validated on a full-scale locomotive traction stand. The implementation was done for a dSPACE DS1103 prototyping board, programmed in Matlab Simulink (the machine code was obtained by compiling the model, using Simulink Coder and dSpace Real Time Interface library - Fig. 2.

Although the actual control system is synthetized in a grouped subsystem, some auxiliary blocks are needed:

- Model input signals, from the power section – the measured quantities from the transducers are acquired by the DS1103 analog to digital converters and made available to the model as Simulink signals by means of the RTI blocks attached to the board hardware resources;
  - The DS1103 analog inputs range is ±10V, so the transducers output signals had been calibrated to this range – yellow Gain blocks in Fig. 2. are used to denormalize the analog measured signals;
- Model output signals to the power section – gating pulses for the power transistors (obtained by the integrated PWM modulator), validation logic signals;
- Local blocks needed for real time control, imposed quantities and interlocks.

Although the inverter is controlled by the DS1103 board, the power inverter has its own local DSP who manages the power system initialization and protection (overcurrent, overvoltage, etc.). This means that some validation signals are exchanged between the DS1103 and the local DSP. A special kind of control signals received by the DS1103 are the signals from the locomotive control panel (containing the torque and speed levers).

The actual field-oriented control simplified algorithm is detailed in Fig. 3. It can be seen that the control system has two validation signals:

- The main validation signal, en, which validates the flux-imposed value and the current controller;
- The secondary validation signal, which validates the speed controller, the torque to active current conversion block (for manual, torque control), and the active current value.

The speed controller is a special proportional-integrative controller whose limits are dynamically adjusted (the upper and lower limits are given by the torque imposing lever.

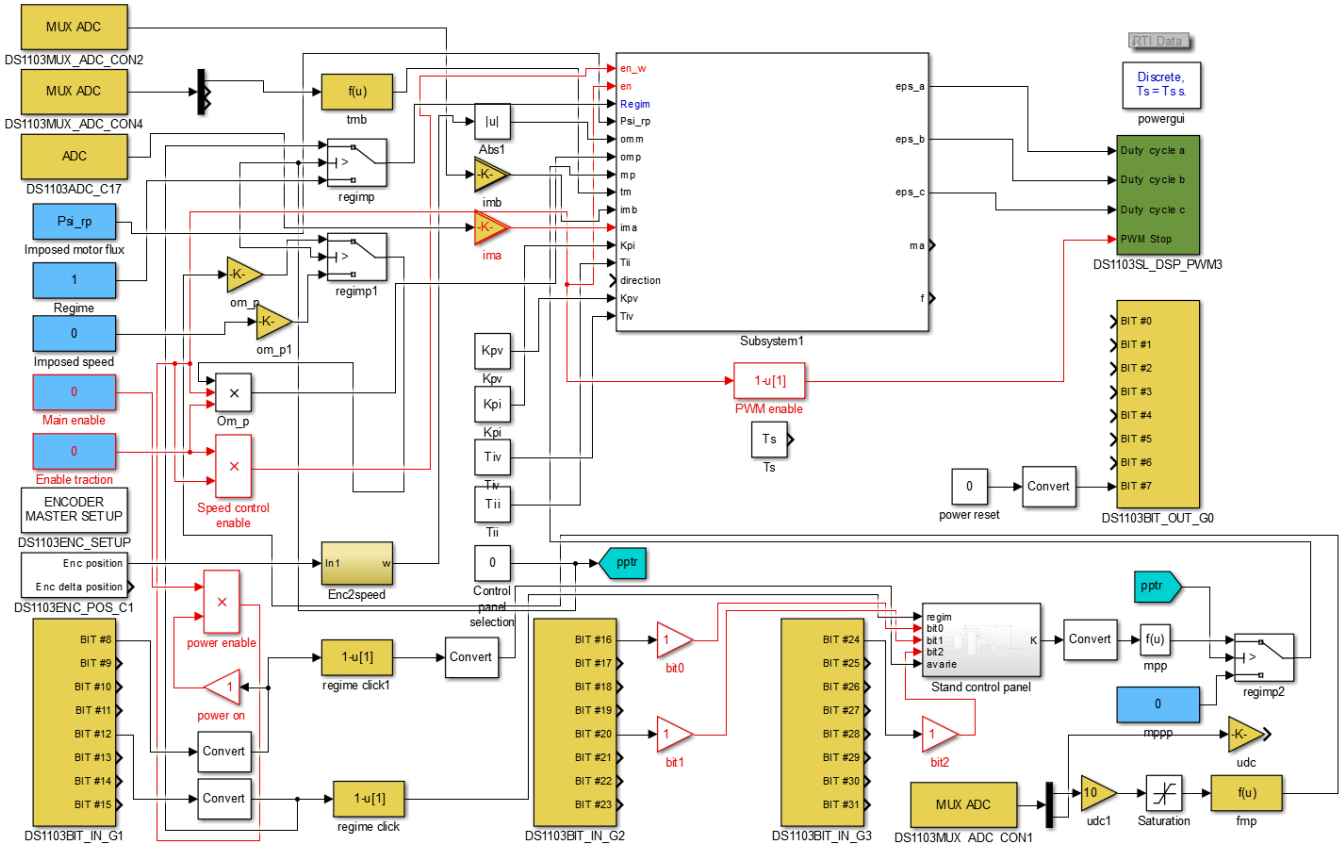

Fig. 2. Experimental Simulink control model

The remaining blocks in the control subsystem are:

- *im abc* - third motor phase current computation block (because only two currents are acquired);
- *Manual mode* - imposed torque to imposed active current conversion block;
- *Motor imposed flux* - gives the real time motor flux as a function of the imposed value, imposed torque and frequency (given the fact that the motor can operate above the rated speed);

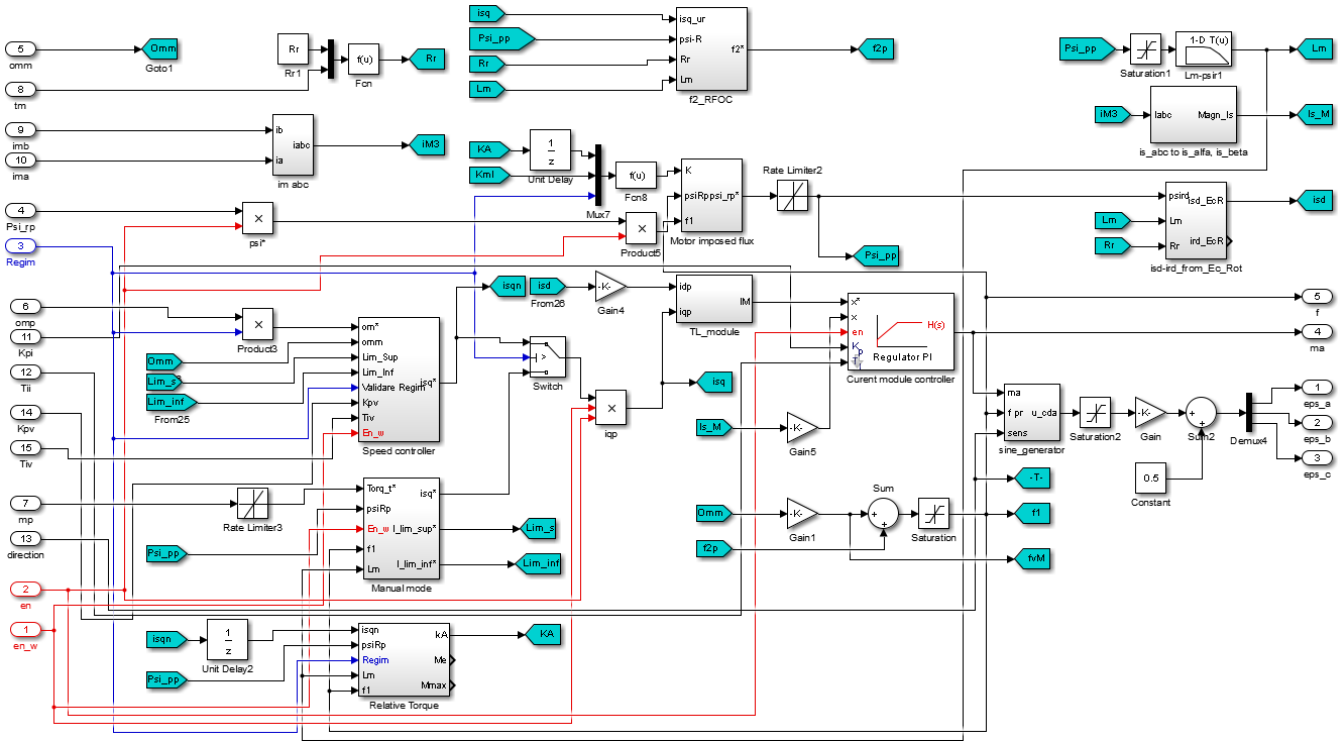

Fig. 3. The simplified field-oriented control system

- *f2_RFOC* - computes the slip frequency;
- *TL_module* - computes the imposed motor current magnitude from the d and q axis currents;
- *is_abc to is_alfa, is_beta* - computes the measured motor current magnitude în the αβ referential;
- *isd-ird_from_Ec_Rot* - gives the imposed magnetizing current for the imposed flux;
- *sine_generator* - software generator of the three phase control signals for the PWM modulator.

The real-time control of the experimental system is done using a virtual control panel, built in ControlDesk NG, which gives the interface between the operator and the Simulink model parameters and signals [9][13]. By modifying the model block parameters, the validation signals and the control system parameters can be modified in real-time. The Simulink model signals can also be displayed on panel meters and virtual scopes.

At the same time, the panel meters are displaying instantaneous model signal values, so in order to virtually measure RMS or mean values, the corresponding quantity computing block is necessary.

The virtual control panel of the experimental traction system, captured during an experiment is illustrated in Fig. 4.

The data displayed on the virtual oscilloscopes was decimated, given the large timespan (75 s), therefore the lower left scope (displaying the three phase duty factors) is distorted. The low rate of change quantities (motor speed, current controller output and the current in the d-q referential) are displayed correctly.

IV. Experimental Setup

The main elements of the experimental stand are:

- Single phase boost rectifier;
- Three-phase traction inverter;
- Three-phase traction motor:
  - U_N = 1400 V, I_N = 576 A, P_N = 1.39 MW;
  - f_N = 62.5 Hz; n_N = 1250 rpm.

The traction inverter is dedicated to the traction motor, so its rated parameters are in accordance. The inverter power source is a single-phase boost rectifier, which can have bidirectional power flow (the braking energy is recovered to the power grid). The DS1103 board controls only the inverter power transistors, the transistors if the boost rectifier are controlled by the power section local DSP (the traction rectifier was used just as power source, the DS1103 board cannot modify the imposed DC-Link voltage, but the work status of the rectifier is controlled by the DS1103 by means of the binary validation signals exchanged with the local DSP).

V. Experimental Results

The experimental protocol considered the following steps:

- The system is initialized (the rectifier is connected to the grid and the DC-Link capacitor is charged to 1800 V);

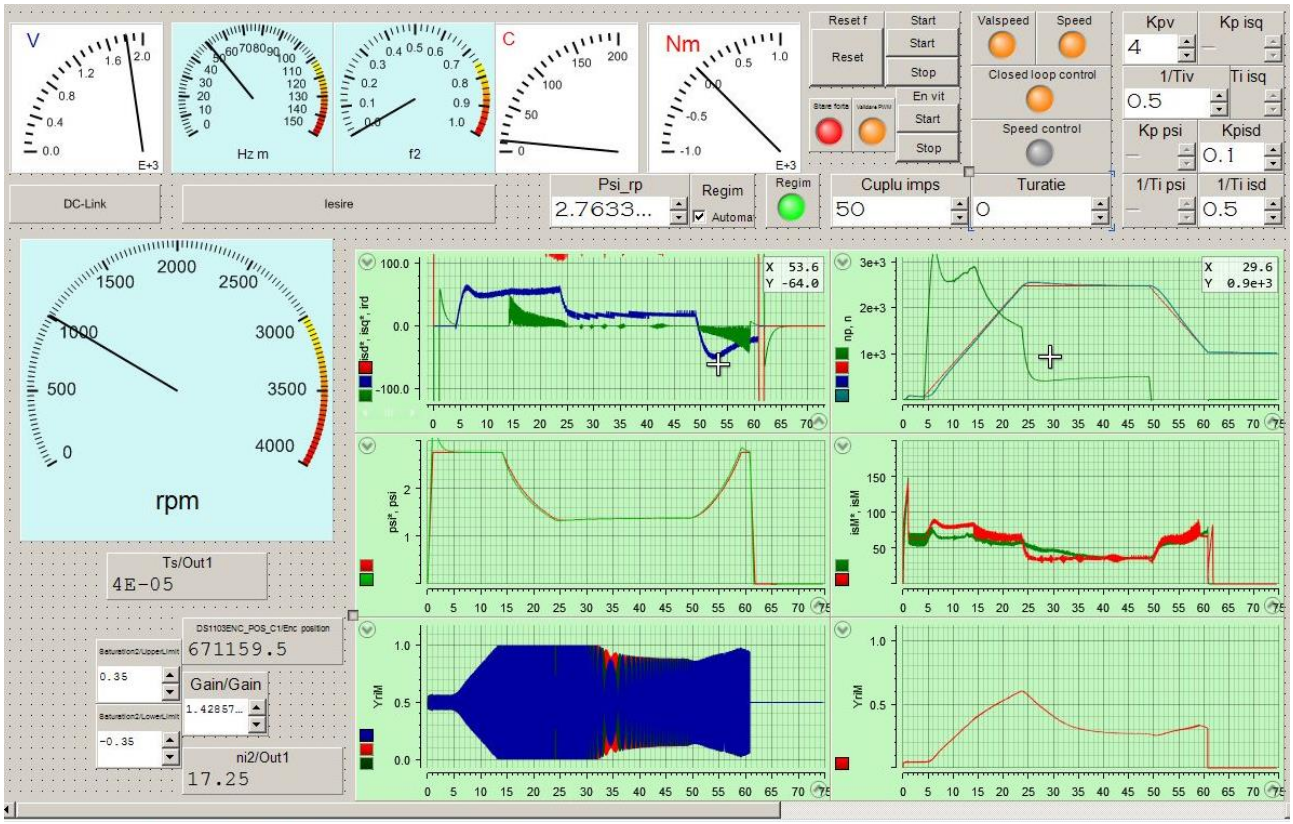

Fig. 4. The experimental traction system control panel

- The motor is magnetized (for this step, only the flux imposing system and the current controller are validated, the imposed torque to active current converter block and the speed controller being inhibited);
- The traction motor is accelerated to 2500 rpm and the stationary regime is obtained;
- The motor is decelerated to 1000 rpm.

The relevant quantities had been recorded by the DS1103 and saved as Matlab workspace file. The recorded signals were subsequently analyzed in Matlab.

As stated, the first step of the experiment consisted in accelerating toe traction motor to twice the rated speed, when the motor is magnetized. For this, the two validation signals are set one by one (the torque and speed subsystems are manually validated when the motor is magnetized. The motor imposed/assumed flux is illustrated in Fig. 5. The imposed flux reaches the steady state value (motor rated flux) in 1 s. For this, the d axis-imposed current is given in Fig. 6. The necessary current in order to obtain 2.76 Wb is 277 A.

After another 3 s, after the motor flux reaches the steady state value, the speed control subsystem is validated, and the first imposed speed of 2474 rpm is established. The imposed speed increases linearly from close to 0 to the steady state value in 20 s. The first interesting thing is that when the motor is only magnetized (the first 4 s of the experiment), although the imposed q axis current is null (Fig. 8.), more than that, the speed control subsystem is inhibited, the motor real speed is not null, but about 72 rpm. The fact that the motor was not driven at this time is further confirmed by the estimated electromagnetic torque, presented in Fig. 9.

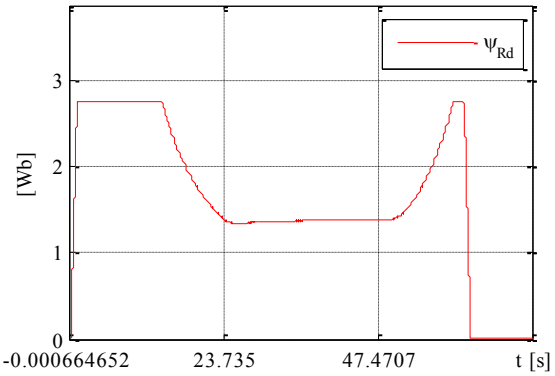

Fig. 5. The motor imposed flux

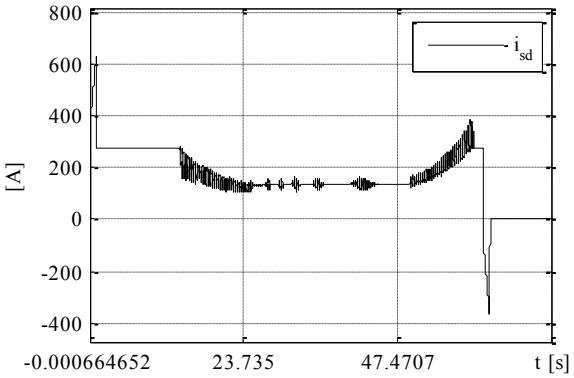

Fig. 6. Imposed d axis current

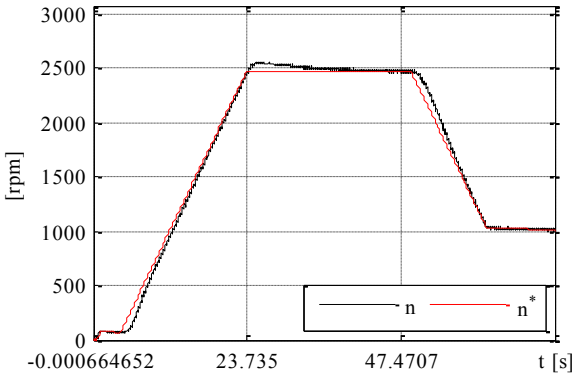

Fig. 7. Motor speed

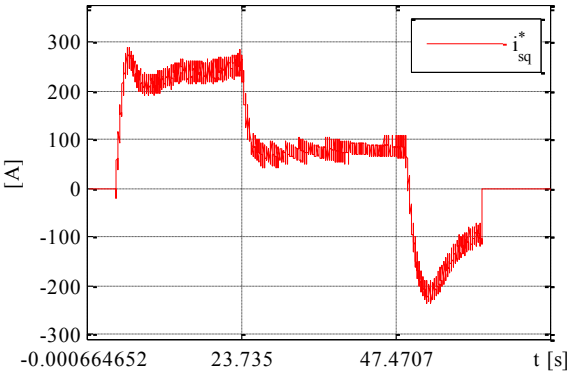

Fig. 8. Motor imposed q axis current

It must be mentioned that the speed controller was designed to have the imposed speed equal to the real speed when the controller is inhibited, so the initial imposed speed is not null, but equal to the real speed of 72 rpm.

The motor speed catches up with the imposed value, although an overshoot of about 3% is noted. An important fact is that the traction motor is driven idle. The steady state q axis current is 75 A. The settling time is about 15 s.

It can be seen that above the motor rated speed, the flux is diminished (the d axis-imposed current is corrected with the speed).

After the steady state regime is settled, the imposed speed is reduced to 1000 rpm. The imposed q axis current becomes negative (as well as the estimated torque), as the motor enters the electromagnetic braking regime. Again, the motor speed follows the imposed speed. The motor estimated flux (given by the d axis current) increases to the motor rated value, as the speed decreases to and bellow the rated speed.

The motor current magnitude is illustrated in Fig. 10. It results that the current control is good, but the current controller is somewhat slow, and the fast transients of the imposed current are missed. Although, the motor performance (respective to the speed) is not affected.

Looking at the current controller output signal (Fig. 11. – the amplitude modulation index), it results that the traction system has sufficient power reserve.

It must be mentioned that at 61th second (experiment time) the system is manually powered off (by resetting the two validation signals).

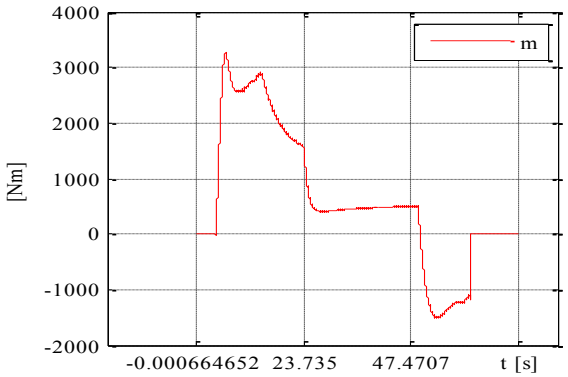

Fig. 9. The estimated electromagnetic torque

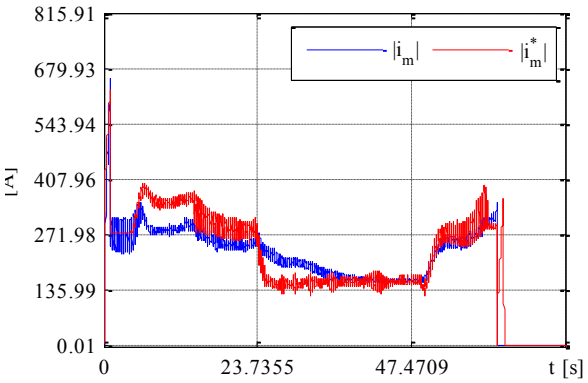

Fig. 10. The motor current magnitude

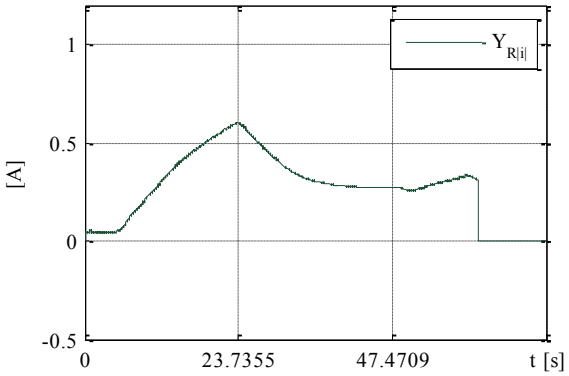

Fig. 11. The current magnitude controller output

CONCLUSIONS

The simplified rotor field-oriented control system was successfully validated on the experimental full scale traction system with good speed regulation results, given the fact that the orientation is only assumed. The filed weakening regime is also obtained with good performance. The DSP sample time for the experiment was 40 µs, but the control algorithm can be used with equally good results with sample times as high as 100 µs. The speed control was good even more so as the idle motor control is difficult. The drawback of the control system is given by the fact that the motor tends to rotate at low speed, when only magnetized, even the fact that the q axis current is null (and the entire speed and torque subsystem is inhibited). This happens also due to the fact that the motor is idle (so the resistant torque is low), which is not the case of a heavy railway vehicle.

Source of research funding in this article: Research program of the Electrical Engineering Department financed by the University of Craiova.

Contribution of authors:
First author – 25%
First coauthor – 25%
Second coauthor – 25%
Third coauthor – 25%

Received on September 28, 2025
Editorial Approval on December 5, 2025

REFERENCES

[1] S. Pancorbo, G. Ugalde, J. Poza and E. A, "Comparative study between induction motor and Synchronous Reluctance Motor for electrical railway traction applications," in 2015 5th International Electric Drives Production Conference (EDPC), Nuremberg, 2015, pp. 1-5, doi: 10.1109/EDPC.2015.7323219.

[2] H. Yamashita, "A traction control method for slip suppression of electric locomotives driven by parallel-connected dual induction motors controlled by one inverter," in 2016 International Conference on Electrical Systems for Aircraft, Railway, Ship Propulsion and Road Vehicles & International Transportation Electrification Conference (ESARS-ITEC), Toulouse, 2016, pp. 1-6, doi: 10.1109/ESARS-ITEC.2016.7841429.

[3] J. Tang, Y. Yang, L. Diao, J. Chen, Y. Chang and Z. Liu, "Parameter identification of induction motors for railway traction applications," in 2018 IEEE Energy Conversion Congress and Exposition (ECCE), Portland, 2018, pp. 284-288, doi: 10.1109/ECCE.2018.8557866.

[4] R. Gomez, L. Pugliese, W. Silva, C. Souse, G. Rezende and F. Rodor, "Speed control with indirect field orientation for low power three-phase induction machine with squirrel cage rotor," *Machines*, vol. 9, no. 12, p. 24, 2021, doi: 10.3390/machines9120320.

[5] M. Ergen and E. Afacan, "Optimizing control of railway traction motor performance with a hardware-in-the-loop method," in 2024 11th International Conference on Electrical and Electronics Engineering (ICEEE), Marmaris, 2024, pp. 101-106, doi: 10.1109/ICEEE62185.2024.10779283.

[6] A. Bitoleanu, M. Popescu and C. Suru, "Experimental performances of the battery charging system of an autonomous locomotive," 2022 22nd International Symposium on Electrical Apparatus and Technologies (SIELA), Bourgas, Bulgaria, 2022, pp. 1-4, doi: 10.1109/SIELA54794.2022.9845794.

[7] CV. Suru, A. Bitoleanu, M. Popescu, M. Linca and F. Ravigan, "Particularities of rotor field orientation control implementation on industrial DSP systems," *Revue Roumaine des Sciences Techniques — Série Electrotechnique et Energétique*, vol. 70, no. 1, 2025, doi: https://doi.org/10.59277/RRST-EE.2025.1.3.

[8] M. Sulaiman, F. Patakor and Z. Ibrahim, "DSP based implementation of field oriented control of three-phase induction motor drives," *IJRET: International Journal of Research in Engineering and Technology*, vol. 2, no. 9, pp. 179-186, 2013.

[9] "DS1103 PPC Controller Board, Features, Release 5.2 – December 2006," dSPACE GmbH, 2006.

[10] M. Linca, C. Suru, M. Popescu and A. Bitoleanu, "Rotor field quasi-oriented control algorithm implementation for railway traction systems on dSPACE DS1103," in 2024 International Conference on Applied and Theoretical Electricity (ICATE), Craiova, 2024, pp. 1-6, doi: 10.1109/ICATE62934.2024.10748608.

[11] M. Popescu and A. Bitoleanu, "New achievements in the rotor field-oriented control for autonomous locomotives: Part 1: System synthesis and theoretical investigations," in 2021 7th International Symposium on Electrical and Electronics Engineering (ISEEE), Galati, 2021, pp. 1-6, doi: 10.1109/ISEEE53383.2021.9628690.

[12] A. Kelemen and M. Imecs, *Field-Oriented Control Systems for Alternating Current Machines*, Bucharest: Academiei, 1989.

[13] "ControlDesk Next Generation Reference For ControlDesk 5.3Release 2014 B – November 2014," dSPACE GmbH, 2014.